Accuracy of a dose-area product compared to an absorbed dose to water at a point in a 2 cm diameter field

Stéphane Dufreneix, Aimé Ostrowsky, Benjamin Rapp, Josiane Daures, jean-marc bordy

Accuracy of a dose-area product compared to an absorbed dose to water at a point in a 2 cm diameter beam

S. Dufreneix, A. Ostrowsky, B. Rapp, J. Daures and J. M. Bordy*

CEA, LIST, Laboratoire National Henri Becquerel (LNE-LNHB), F-91191 Gif-sur-Yvette, France

*E-mail: jean-marc.bordy@cea.fr

Purpose: Graphite calorimeters with a core diameter larger than the beam can be used to establish dosimetric references in small fields in terms of dose-area product (DAP). The DAP can theoretically be linked to the absorbed dose at a point, *D*, by the determination of a "profile correction". This study is aimed at comparing DAP and absorbed dose at a point in a 2 cm diameter beam for which both references exist.

Method: Two calorimeters were used, respectively with a sensitive volume of 0.6 cm (for the absorbed dose at a point measurement) and 3 cm diameter (for the DAP measurement). The "profile correction" was calculated from a 2D dose mapping using three detectors: a PinPoint chamber, a synthetic diamond and EBT3 films. A specific protocol to read EBT3 films was implemented and the dose-rate and energy dependences were studied to assure a precise measurement, especially in the penumbra and out-of-field regions.

Results: EBT3 films were found independent on dose rate over the range studied but showed a strong under-response (18%) at low energies. Depending on the dosimeter used for calculating the "profile correction", a deviation of 0.8% (PinPoint chamber), 0.9% (diamond) or 1.9% (EBT3 films) was observed between the calibration coefficient derived from DAP measurements and the one directly established in terms of absorbed dose to water at a point.

Conclusion: The DAP method can currently be linked to the classical dosimetric reference system based on absorbed dose at a point with a confidence interval of 95% ($k = 2$). None of the detectors studied can be used to determine an absorbed dose to water at a point from a DAP measurement with an uncertainty smaller than 1.2%.

Keywords: *small fields, dose-area product, EBT3, dosimetric references*

1. Introduction

In high energy X ray beams, lateral electronic equilibrium cannot be reached if the size of the beam is smaller than the practical range of secondary electrons[1]. That is to say, in a 6 MV beam, for beam sizes lower than 2.6 cm diameter because the minimal radius needed to achieve complete lateral

electronic equilibrium is[2] 1.3 g cm^{-2}. For such a small field, absorbed dose at a point at the center of the beam is not traceable to references established in beams larger than the particle range of secondary electrons[3]. Many dosimeters have a size close to the smallest beam size used in clinical radiotherapy beams (4 mm)[4,5]. A formalism was introduced[1] in 2008 for reference dosimetry of small and non-standard fields, based on the determination of a correction factor $k_{Q_{msr},Q}^{f_{msr},f_{ref}}$ for such small dosimeters. Numerous studies have determined this correction factor for some detectors by Monte Carlo simulations and by measurements[6-9], allowing reference measurements for small fields in radiotherapy departments. To avoid using such a correction factor, another method based on a dose-area product (DAP)[10] by using dosimeters larger than the beam section is possible[11,12].

Recently, this method was used in a primary laboratory to establish dosimetric references in small fields[13,14]. Dosimetric references were established in terms of DAP in circular beams of 2, 1 and 0.75 cm diameter using a 3 cm core diameter graphite calorimeter as primary dosimeter and a plane parallel ionization chamber with the same sensitive surface as transfer dosimeter. A standard uncertainty smaller than 0.9% on the calibration coefficient of the plane parallel ionization chamber was achieved.

As dosimetric references established in small fields in terms of DAP are not used for the commissioning of the current treatment planning systems (TPS), DAP need to be converted in terms of absorbed dose to water at a point, as recommended by the IAEA TRS398 dosimetry protocol[15]. A conversion coefficient is then needed to determine the absorbed dose delivered at a point from the DAP references obtained with a primary dosimeter such as the specially designed graphite calorimeter of LNE-LNHB. The conversion coefficient can be determined by a 2D dose mapping of the beam over the sensitive surface of the primary dosimeter. Precise measurements are especially required in the penumbra region (80%-20% of the absorbed dose deposited on the axis) and the out-of-field region (20%-0% of the absorbed dose deposited on the axis) where the beam energy and dose-rate vary drastically[3].

Radiochromic films such as EBT3 films (Ashland Specialty Ingredients, Bridgewater, NJ, USA) are commonly used for 2D dose distribution measurements[16-18]. They are also suitable for measurements in small fields[19,20] due to their high spatial resolution and water equivalence.

This study presents the commissioning that was realized for EBT3 films. A dose-rate and an energy dependence studies were conducted. Dose distributions were measured in small circular beams of 2, 1 and 0.75 cm diameter and compared to other dosimeters. The accuracy of the DAP technique was evaluated in the 2 cm diameter beam by comparing a dosimetric reference directly established in terms of absorbed dose to water at a point and the one derived from a DAP measurement coupled with a conversion coefficient.

2. Theory

2.1. DAP proprieties

The DAP represents the energy deposited by the beam over the sensitive surface of the detector and is expressed in Gy.cm². It can be interpreted as the integral of the absorbed dose to water profile, $D_w(r)$, over the sensitive surface of the detector, such as for a circular beam:

DAP = $\int_r 2\pi r D_w(r)\, dr$. Where r the off axis distance.

As a consequence, the contribution to the DAP depends on the absorbed dose to water along the profile and the off-axis distance (figure 1). Thus, even if the highest dose is deposited on the axis, its contribution to the DAP is null ($r = 0$). On the contrary, out-of-field doses cannot be neglected because the highest contribution of an irradiation beam to DAP is within the penumbra between 0.8 and 1.1 cm for a beam of 2 cm diameter as shown in figure 1.

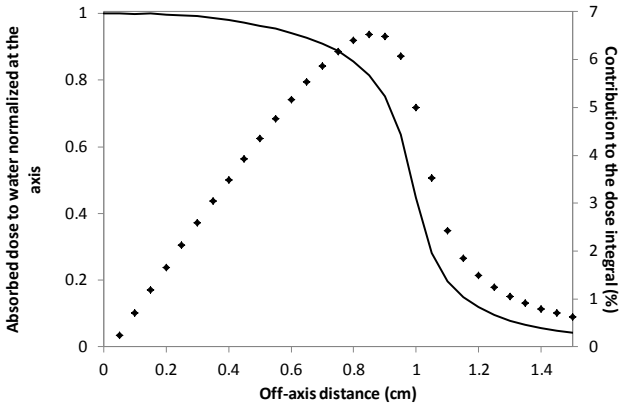

Figure 1 : variation of the absorbed dose with the off-axis distance and its corresponding contribution to the dose integral in a 2 cm diameter beam.

The DAP is already widely used in radiology as it was shown approximately invariant in air with distance, d, from the focal spot[21] since the surface increases with the square of d while the dose decrease with the square of d. The main differences with the use of DAP suggested here for small beams of radiotherapy is the surface which is smaller, up to about 3 cm² (for a beam diameter of 2 cm), than for radio diagnosis and the medium, water instead of air which leads a huge difference in terms of scattered radiation between radio diagnosis and radiotherapy.

2.2. Determination of the "profile correction"

An absorbed dose delivered at a point can be derived from a DAP measurement by applying a conversion coefficient based on the measurement of the beam profile, called conversion coefficient in the following, which takes into account the inhomogeneity of the dose deposition over the sensitive surface of the primary dosimeter. It can be expressed as:

$$k_{prof} = \frac{g(0).\int_0^R rdr}{\int_0^R g(r)rdr}$$

where *gD(0)* is the absorbed dose at a point on the axis, $2\pi \int_0^R rdr$ is the sensitive surface of the calorimeter used for the primary measurement - R being the radius of the calorimeter, *gD(r)* is the

absorbed dose at a distance r from the axis and $2\pi \int_0^R g(r) r dr$ is the dose integral over the sensitive surface of the calorimeter. As a consequence, the establishment of a dosimetric reference in terms of absorbed dose at a point based on a DAP measurement requires:

- an absolute DAP measurement with a large section graphite calorimeter
- a two dimensions dose mapping of the beam. If a cylindrical symmetry can be assumed, only a hemi-profile is needed.

3. Materials and method

Unless otherwise stated, all uncertainties are given for $k = 1$. In agreement with the Guide to the Expression of Uncertainty in Measurement[22], the number in parentheses after a value is the numerical value of the combined standard uncertainty referred to the corresponding last digits of the quoted result.

3.1. Facilities

Dose rate dependence of EBT3 films was investigated in a 10 cm x 10 cm field at 6 MV ($TPR_{20,10}$ = 0.675) on a Saturne 43 linear accelerator (General Electric). Unlike most dose rate dependence studies, the pulse frequency was left unchanged (200 Hz) but the number of electrons entering the acceleration section was tuned. Thus, this is more representative of the dose rate change that occurs when measuring a dose profile far from the central axis. Doses of 5 Gy were delivered at 10 g cm^{-2} for each dose rate (from 0.018 to 1.83 mGy per pulse).

Energy dependence was studied in the beams described in table 1 delivered by the Saturne 43, a ^{60}Co irradiator (Cirus/Alcyon, CIS Bio) and a low energy X-ray generator equipped with a SEIFERT 320 kV ISOVOLT HS tube. The 6 medium-energy X-ray beams were chosen among existing norms and protocols (IEC: International Electrotechnical Commission[23]; CCRI: Consultative Committee for Standards of Ionizing Radiations[24]; ISO International Organization for Standardization[25]). For each beam quality, dosimetric references in terms of absorbed dose to water are available at LNE-LNHB[26]. The same dose rate (0.208 (2) Gy min^{-1}) was used for all the beams. Irradiations took place in reference conditions and measurements were realized at 10 g cm^{-2} for the linear accelerator, 5 g cm^{-2} for the ^{60}Co and 2 g cm^{-2} for the low/medium energy beams. All measurements were realized in a water phantom. A dose of 5 Gy was delivered to 2 EBT3 films at the reference depth.

Name	RQR6	RQR9	RQR10	CCRI180	CCRI250	ISO300	Co^{60}	6 MV	12 MV
Mean energy (MeV)	0.044	0.056	0.063	0.085	0.120	0.141	1.25	*2*	*4*

Table 1: Mean energy of the beams (medium energy X-rays and high energy photons) used for the energy dependence.

Measurements in the 2 cm diameter beam were conducted on the Saturne 43 equipped with an additional collimator 10 cm long made of tungsten. Jaws delimited a rectangular beam on the collimator entrance which allowed the irradiation of a monitor chamber placed between the irradiation head and the additional collimator. A precise alignment of the conical hole of the collimator and the beam axis was achieved by using a specific support, validating the hypothesis of a cylindrical beam. Profile

measurements with the EBT3 films and with 1D dosimeters over 4 axis separated by 45° confirmed the accuracy of the alignment by the quality of the symmetry.

3.2. Detectors used

For all the standard beams used in the dose-rate and energy studies, a NE_2571 chamber was used for reference dosimetry. Its calibration coefficient was directly determined from calorimetric measurements.

In the 2 cm diameter beam, a small graphite calorimeter (named GR10) of 0.6 cm core diameter[27] was used to establish a dosimetric reference directly in terms of an absorbed dose to water at a point. A large graphite calorimeter (named GR11) with a 3 cm core diameter was used for primary measurements in terms of DAP[14]. Calorimeters were used in quasi-adiabatic mode. Measurements were conducted in a 30 cm x 30 cm x 20 cm graphite phantom with the center of the core located at 100 cm from the source and 10 g cm^{-2} depth. For a better statistic, at least 85 calorimetric measurements were realized, all corrected from the monitor.

For both calorimeters, the conversion coefficient was determined using EBT3 film measurements as well as 1D detectors (assuming a cylindrical symmetry): a PTW_31014 PinPoint ionization chamber and a synthetic diamond developed at CEA-LCD[28,29] (table 2). The PinPoint chamber and the diamond were pre-irradiated for 10 min before all measurements. Two quick profiles were measured along two perpendicular axes for centering. For the final profile measurement, the signal was integrated over 10 s at each point. The longitudinal axis of the detectors was positioned parallel to the beam in order to offer the best spatial resolution. For the diamond dosimeter, a leakage current of around 1% of the signal measured on the beam axis was observed and taken into account.

Name	Type	Dimensions
NE_2571	Ionization chamber	length: 0.241 cm; diameter: 0.63 cm
GR10	Graphite calorimeter	diameter: 0.6 cm; thickness: 0.6 cm
GR11	Graphite calorimeter	diameter: 3 cm; thickness: 0.3 cm
PTW_31014	Ionization chamber	length: 0.5 cm; diameter: 0.2 cm
LCD_Diamond	Synthetic diamond	0.1 x 0.1 x 0.0165 cm

Table 2: Characteristics of the dosimeters used in this study.

3.3. Protocol for EBT3 films

EBT3 films from lot A12151101 were used. Each sheet of 20.3 x 25.4 cm² was cut in 20 square-films of 5 cm size. Care was taken when manipulating EBT3 films to avoid soiling and to limit light exposure as much as possible. They were marked to keep the same landscape orientation during scanning. An Epson Perfection V750 Pro A4 in 48-bit color mode was used without applying any image correction. For a better reproducibility in the EBT3 film position, a slide holder was used. Due to the small size of the EBT3 films, the heterogeneity of the scanner can be neglected[30]. Images were saved in TIFF format and analyzed with an in-house program using Root libraries (European Organization for Nuclear Research, CERN) and ImageJ (National Institutes of Health). Even though some studies suggested a multichannel dosimetry protocol[11], only the red channel was extracted. Since spatial resolution is of major concern in small fields, a resolution of 360 dots per inch was selected so that the pixel size is smaller than 0.1 mm. This small resolution is however linked to an increase in the statistical uncertainty[31].

Some authors[32-33] have suggested that the response of EBT film could depend on the reading system's temperature. A thermistor BR14 (General Electric) was thus stuck between two EBT3 films to record the temperature of the scanner bed. Measurements showed that a warm up of 5 blank scans lead to a temperature rise of approximately 1 °C and that the temperature increased of several degrees during multiple scanning (up to 8 °C for 80 scans). No impact on the raw pixel value was found, within the statistical uncertainty of 0.5%. However, the first scan of each EBT3 film gave systematically a raw pixel value 0.7% lower than the three others. This was attributed to the temperature of the EBT3 film which changes from room temperature (19 °C) to the scanner temperature. Only the mean of the three last scans was therefore considered.

EBT3 films were scanned prior to the irradiation to get the unexposed intensity (I_{unexp}) and for practical reasons, scanned a week after the irradiation to get the exposed intensity (I_{exp}). The deviation of I_{exp} with time was studied between 4 and 32 days after the irradiation but the maximum deviation found was of 0.8% and no trend was observed.

The net optical density was calculated using the following formula[34]:

$$\boldsymbol{netOD = OD_{exp} - OD_{unexp} = log_{10}\left(\frac{I_{unexp} - I_{bckg}}{I_{exp} - I_{bckg}}\right)}$$

where I_{bckg} is the background intensity equals to 65535 as measured on the images of the slide holder. Measured reproducibility for the protocol was of 0.55% in terms of net optical density, *netOD*, for 20 EBT3 films coming from the same sheet and irradiated at 4 Gy on a ^{60}Co unit in a 10 cm square beam.

A calibration curve was measured to convert the *netOD* into absorbed dose. The uncertainty on the absorbed dose delivered to the EBT3 film was between 1.0 and 2.1% depending on the beam studied. The uncertainty on *netOD* decreased with dose and was comprised between 1 and 2%. The following formula[35] was used for the fit:

$$\boldsymbol{D_{fit} = a.netOD + b.netOD^n}$$

where a, b and n are adjustable parameters. The n value is specific to a protocol[36] and in our case the best fit was observed for n = 3.8.

For measurements in the 2 cm diameter beam, three EBT3 films were successively irradiated and the mean was considered to decrease the statistical noise.

3.4. Monte Carlo simulations

A parallel version of PENELOPE 2006[37] was used to simulate spectra at different distances from the axis in the 2 cm diameter beam. The Saturne 43 head was modeled and the initial parameters of the electrons were determined: mean energy, spectral dispersion and spatial dispersion. These parameters were adjusted by comparing the lateral and depth dose variations simulated to measurements. The following parameters were selected for simulations in the treatment head: E_{abs}(photons) = 5 keV, E_{abs}(electrons) = E_{abs}(positons) = 50 keV, C_1 = C_2 = 0.05, W_{cc}=W_{cr}= 10 keV. Dose profiles were measured with a PinPoint PTW_31014 ionization and EBT3 films. Depth dose variations were measured with an Exradin A1SL. Depth dose variations were also measured with a home-made parallel-plate ionization chamber[14] larger than the beam because it is less sensitive to a drift of the chamber center from the beam axis when depth increases. For the simulation of lateral and depth dose variation, the voxel size was adjusted to the sensitive volume of the detector used during measurements so that the averaging effect could be taken into account and a direct comparison could be performed. All modeled distributions passed a global gamma analysis with a 0.5%/1 mm criteria.

Once the initial parameters were adjusted, 3.4 10^9 primary showers were simulated and a phase space file (PSF) was created at the lower part of the additional collimator. The 2.3 10^8 particles of the PSF were used to simulate spectra at 10 g cm^{-2} in water with an energy sampling of 37.5 keV. Three spectra were simulated: one in a 2 mm radius circle on the axis, one in a ring of 2 mm wide between 0.9 and 1.1 cm from the axis (penumbra region) and one in a ring of 2 mm wide between 1.4 and 1.6 cm from the axis (out-of-field region).

4. Results and discussion

4.1. Dose rate dependence

Raw results show a strong over-response at low dose rates (crosses in figure 2). However, delivering 5 Gy with the smallest dose rate took approximately 4 h during which water could interact with the film. To quantify this influence, the same absorbed dose was delivered to 8 films but the time spent in water varied from a few minutes to 4 h. Results showed in figure 3 suggest that the net optical density increases with the time spent in water (+0.4% per hour). By applying a linear correction on the raw dose rate results, EBT3 films can be considered independent on dose rate over the range studied. The uncertainty for the corrected data was dominated by the uncertainty of the linear correction (6.5%). Care should thus be taken when EBT3 films remain more than 30 min in water.

Accuracy of a dose-area product compared to an absorbed dose to water at a point in a 2 cm diameter beam

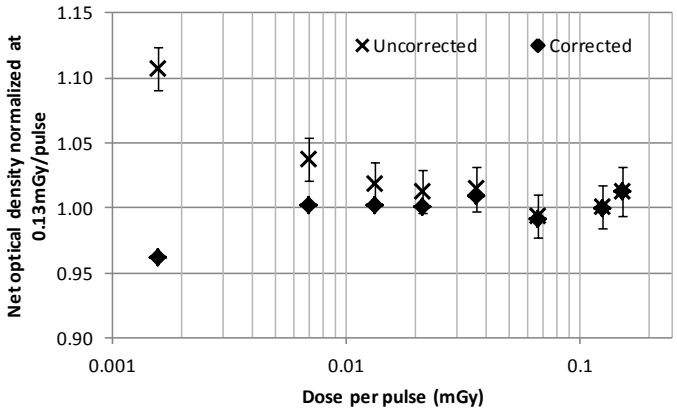

Figure2: Net optical density variation with the absorbed dose rate. Uncertainty on corrected data (6.5%) was not plotted for clarity.

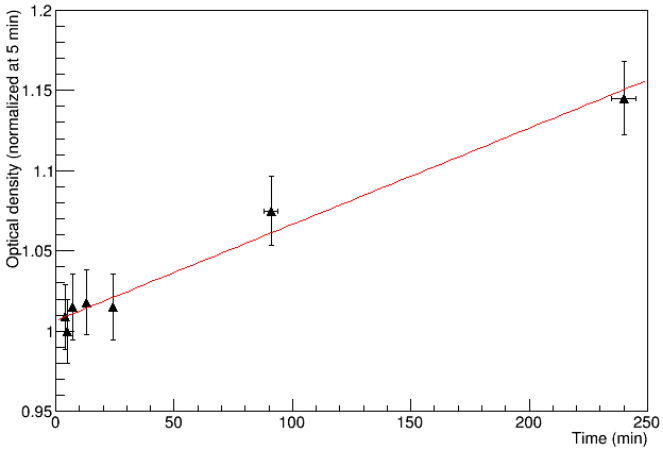

Figure 3: Net optical density variation with the time spent in water.

4.2. Energy dependence

Results given in figure 4 show a strong under-response at low energies (down to 18%). The same trend was observed in other studies[38,39]. Calibration curves represented in figure 5 and measured in RQR10, CCRI250, ^{60}Co and 6 MV beams show that the under-estimation is dose independent: the net optical density measured in the RQR10 beam is always 13% lower than the one measured in the ^{60}Co or the 6 MV beam (respectively 5% for the CCRI250).

Accuracy of a dose-area product compared to an absorbed dose to water at a point in a 2 cm diameter beam

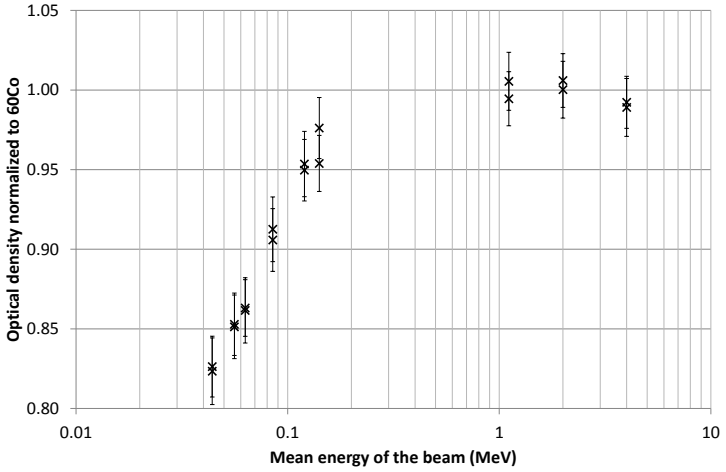

Figure 4: Net optical density variation with the mean energy of the beam.

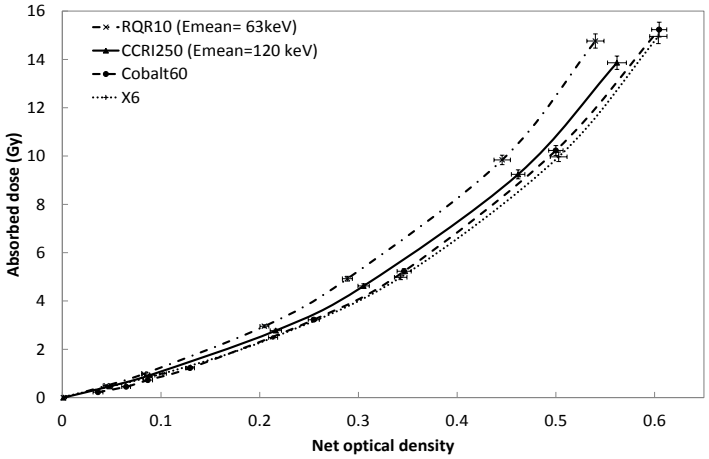

Figure 5: Calibration curves for different beam qualities.

Spectra simulated at different distances from the axis in a 6 MV circular beam of 2 cm diameter are shown in figure 6 with a log scale. Because the major contributors to the dose in close proximity of the field edge come from the collimator and patient scatters[40], the proportion of low-energy photons increases with the distance to the beam axis. However, the proportion of photons with an energy lower than 200 keV over a 3 cm diameter surface is only 2.6% in the 2 cm diameter. This introduces a systematic error smaller than 0.5% on the determination of the dose integral.

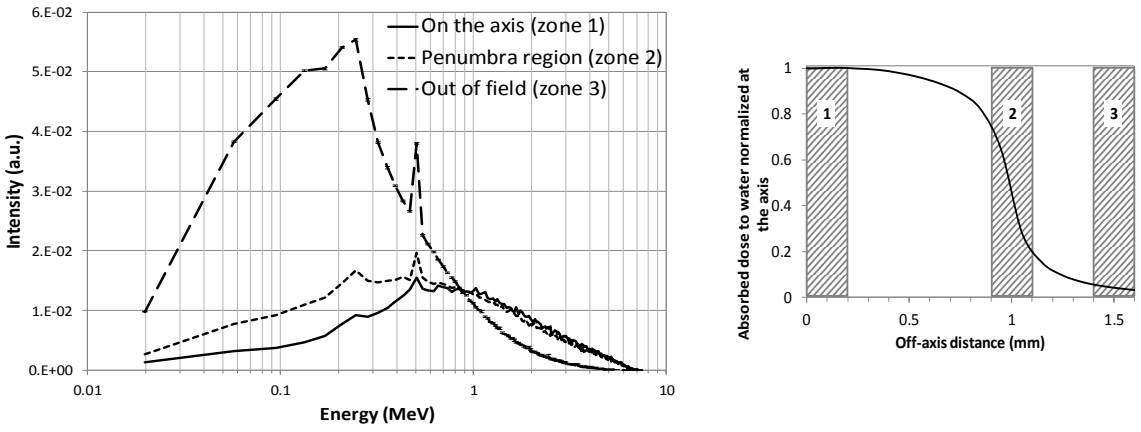

Figure 6 : left: simulated spectra in different regions (represented on the right) in a 6 MV circular beam of 2 cm diameter (log scale). Uncertainty bars are plotted only for the out-of-field spectra for better clarity.

4.3. k_{prof} values

Two series of measurements (named "set A" and "set B") were conducted several months apart with the whole experiment disassembled in between. Results obtained with the PinPoint chamber, the synthetic diamond and EBT3 are given in table 3. The type B uncertainty was determined by calculating k_{prof} from different profiles for the point dosimeters and by considering the standard deviation of the results over the three EBT3 films. No uncertainty was taken into account for the energy dependence. It was estimated to 0.5% for the EBT3 but should be higher for the diamond dosimeter and lower for the PinPoint chamber. No uncertainty was added to the point dosimeters for the cylindrical geometry hypothesis.

		Ø = 0.6 cm		Ø = 3 cm	
		k_{prof}	**Relative uncertainty**	**k_{prof}**	**Relative uncertainty**
Set A	PTW_31014	1.0052 (22)	0.22%	2.215 (13)	0.58%
	LCD_Diamond	1.0033 (29)	0.29%	2.214 (17)	0.78%
	EBT3	1.0051 (71)	0.71%	2.240 (17)	0.74%
Set B	PTW_31014	1.0052 (21)	0.21%	2.234 (26)	1.17%
	LCD_Diamond	1.0038 (30)	0.30%	2.231 (37)	1.65%
	EBT3	1.0033 (80)	0.80%	2.267 (16)	0.70%

Table 3: Conversion coefficient values determined with different dosimeters in the 2 cm diameter beam at 6 MV. Uncertainty is given at k = 1.

As expected, k_{prof} is smaller when the diameter is smaller than the beam section, . All $k_{prof}(Ø=0.6\ cm)$ are in agreement within the uncertainties for each set. The higher uncertainty on the EBT3 film value is due to statistical noise. When the surface of interest is larger than the beam section, the conversion coefficient reaches 2.2 because the dose distribution is strongly heterogeneous over the considered area including the penumbra and a part of the out of beam region. All $k_{prof}(Ø=3\ cm)$ are in agreement within the uncertainties for each set but large deviations are observed between the dosimeters.

One can also notice that the $k_{prof}(Ø=3\ cm)$ values of set B are systematically higher than the values of set A which is linked to the reproducibility of the experiment: 0.9% for the PinPoint, 0.8% for the LCD_Diamond and 1.3% for the EBT3. The relative position of the $k_{prof}(Ø=3\ cm)$ values for the different dosimeters is nonetheless unchanged. The uncertainties for the point dosimeters are also higher because the beam was slightly elliptical for set B (0.3 mm difference on the beam width between the horizontal and vertical profiles). The reproducibility of DAP measurements are thus much more sensitive to the shape of the beam than if an absorbed dose at a point is considered (reproducibility inferior to 0.2%).

4.4. Accuracy of the conversion from DAP to D

Using a small graphite calorimeter of 0.6 cm diameter and the $k_{prof}(Ø=0.6\ cm)$ described above, a calibration coefficients in terms of absorbed dose at a point N_{Dwref} could be determined in 2 cm

diameter beam at 6 MV. Using a large graphite calorimeter of 3 cm diameter and the $k_{prof(Ø=3\ cm)}$ described above, another calibration coefficients, derived from DAP measurements could be determined in terms of absorbed dose at a point. Calorimetric measurements were made during set A so only the corresponding k_{prof} values are considered here.

The comparison of these two calibration coefficients in terms of absorbed dose to water at a point is given in figure 8.

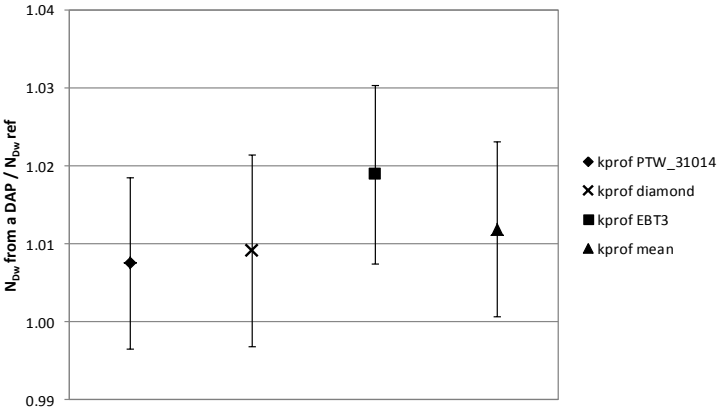

Figure 8: Comparison of the calibration factors in terms of absorbed dose to water determined in the 2 cm diameter beam from a small and a large calorimeter measurements at 6 MV.

Depending on the dosimeter used for the determination of the conversion coefficient, the deviation between the two calibration coefficients is of 0.8% for the ionization chamber, 0.9% for the diamond or 1.9% for the EBT3. However, no ideal dosimeter was found for a precise determination of the conversion coefficient: as shown in Figure 9, the PinPoint chamber has a sensitive volume too large for an accurate profile measurement. It was difficult to account for the leakage current of the diamond dosimeter and if no correction was applied for the leakage current $k_{prof(Ø=3\ cm)}$ value can change for 1.2% in the 2 cm diameter beam. As for EBT3, the deviation between the calibration coefficients is surprisingly high and cannot be attributed to the energy or the dose-rate dependence. By considering the mean value of the $k_{prof(Ø=3\ cm)}$ from the three dosimeters, the two calibration coefficients differ from 1.19% with an uncertainty of 1.13% (k = 1). The DAP method can thus be linked to the classical dosimetric reference system with a confidence interval of 95% (k = 2).

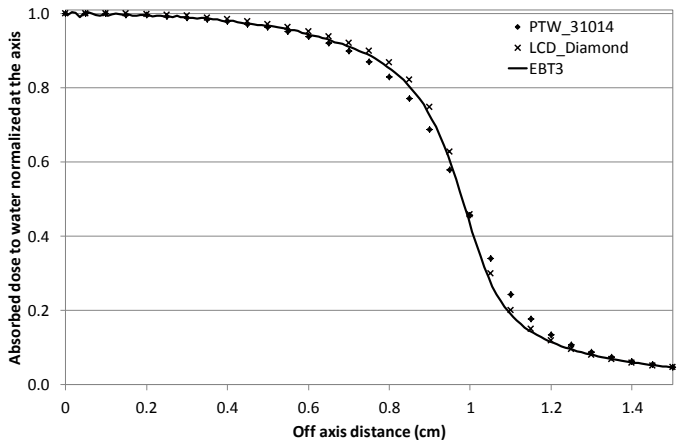

Accuracy of a dose-area product compared to an absorbed dose to water at a point in a 2 cm diameter beam

Figure 9: Dose profiles measured in water at 10 g cm^{-2} depth with different dosimeters in a 2 cm diameter beam at 6 MV.

More profile measurements are planned with other dosimeters like the synthetic diamond PTW_60019, a stereotactic diode or the scintillator W1 in order to improve the comparison and to decrease the uncertainty on the $k_{prof}(Ø=3\ cm)$. Using such commercially available detectors for which $k_{Q_{msr},Q}^{f_{msr},f_{ref}}$ factors are available and close to 1 in small circular beams would also enable comparing the DAP method to the classical dosimetric reference system in the 1 and 0.75 cm diameter beams.

5. Conclusion

EBT3 films were found independent of dose rate but show a strong under-response at low energies. In agreement with a synthetic diamond dosimeter previously validated, they appear as good candidates for the measurement of the 2D dose distribution in small fields. It was also highlighted that a precise determination of a conversion coefficient for a surface larger than the beam section is difficult. As a consequence, the transfer of a DAP based calibration coefficient in terms of absorbed dose at a point will significantly increase the uncertainty because of the 1.2% difference between the DAP method and the classical dosimetric reference system. Further investigations are under way for a more precise measurement of dose profile and conversion coefficients in small beams by using other dosimeters. Once this difficulty is overcome, the dosimetric references available at the LNE-LNHB in terms of DAP in small beams of 2, 1 and 0.75 cm diameter could be transferred to radiotherapy departments in terms of absorbed dose to water at a point allowing a direct traceability to an absorbed dose primary standard specially designed for small fields.

References

[1]R. Alfonso, P. Andreo, R. Capote, M. Saiful Huq, W. Kilby, P. Kjall, T. R. Mackie, H. Palmans, K. Rosser, J. Seuntjens, W. Ullrich, and S. Vatnitsky, "A new formalism for reference dosimetry of small and nonstandard fields", *Med. Phys.* **35,** 5179 (2008).

[2]X. Li, M. Soubra, M. Szanto and L. H. Gerig, "Lateral electron equilibrium and electron contamination in measurements of head-scatter using minihantoms and brass caps", *Med. Phys.* **22**, 1167 (1995).

[3]I. P. E. M. "Small field MV photon dosimetry", Report 103, Institute of Physics and Engineering in Medicine (2010).

[4]A. Chalkley and G. Heyes, "Evaluation of a synthetic single-crystal diamond detector for relative dosimetry measurements on a CyberKnife™." Br J Radiol **87**, 20130768 (2014).

[5]P. Mancosu, G. Reggiori, A. Stravato, A. Gaudino, F. Lobefalo, V. Palumbo, P. Navarria, A. Ascolese, P. Picozzi, M. Marinelli, G. Verona-Rinati, S. Tomatis and M. Scorsetti, "Evaluation of a synthetic single-crystal diamond detector for relative dosimetry on the Leksell Gamma Knife Perfexion radiosurgery system", *Med. Phys.* **42**, 5035 (2015).

[6]H. Benmaklouf, J. Sempau and P. Andreo, "Output correction factors for nine small field detectors in 6 MV radiation therapy photon beams: A PENELOPE Monte Carlo study", *Med. Phys.* **41**, 041711 (2014).

[7]P. Francescon, W. Kilby and N. Satariano, “Monte Carlo simulated correction factors for output factor measurement with the CyberKnife system—results for new detectors and correction factor dependence on measurement distance and detector orientation”, *Phys. Med. Biol.* **59**, N11 (2014).

[8]J. M. Larraga-Gutierrez, "Experimental determination of field factors ($\Omega_{Q_{clin},Q_{msr}}^{f_{clin},f_{msr}}$) for small radiotherapy beams using the daisy chain correction method", *Phys. Med. Biol.* **60**, 5813 (2015).

[9]T. S. A. Underwood, B. C. Rowland, R. Ferrand and L. Vieillevigne, "Application of the Exradin W1 scintillator to determine Ediode 60017 and microDiamond 60019 correction factors for relative dosimetry within small MV and FFF fields", *Phys. Med. Biol.* **60**, 6669 (2015).

[10]T. S. A. Underwood, H. C. Winter, M. A. Hill, and J. D. Fenwick, " Detector density and small field dosimetry: Integral versus point dose measurement schemes", *Med. Phys.* **40**, 082102 (2013).

[11]A. Djouguela, D. Harder, R. Kollhoff, A. Ruhmann, K. C. Willborn and B. Poppe, “The dose-area product, a new parameter for the dosimetry of narrow photon beams” *Z. Med. Phys.* **16,** 217-227 (2006).

[12]F. Sanchez-Doblado, G. H. Hartmann, J. Pena, J. V. Rosello, G. Russiello and D. M. Gonzalez-Castano, “A new method for output factor determination in MLC shaped narrow beams”, *Phys. Med.* **23,** 58-66 (2007).

[13]A. Ostrowsky, J-M. Bordy, J. Daures, L. De Carlan, F. Delaunay, “Dosimetry for small size beams such as IMRT and stereotactic radiotherapy. Is the concept of the dose at a point still relevant? Proposal for a new methodology”, *CEA Report*, R-6243 (2010). Available at: http://www.nucleide.org/Publications/CEA-R-6243_PDS.pdf

[14]S. Dufreneix, A. Ostrowsky, M. Le Roy, L. Sommier, F. Delaunay, B. Rapp, J. Daures and J-M. Bordy, “Using a dose-area product for absolute measurements in small fields: a feasibility study” *Phys. Med. Biol.* **61**, 650-662 (2015).

[15]IAEA, “Absorbed Dose Determination in External Beam Radiotherapy: An International Code of Practice for Dosimetry on Standards of Absorbed Dose to Water,” Technical Reports Series No. 398, International Atomic Energy Agency (2006).

[16]M. J. Butson, P. K. N. Yua, T. Cheung and P. Metcalfe, "Radiochromic film for medical radiation dosimetry", *Mater. Sci. Eng.* **41**, 61-120 (2003)

[17]C. Fiandra, M. Fusella, F. Romana Giglioli, A. Riccardo Filippi, C. Mantovani, U. Ricardi and R. Ragona, “Comparison of Gafchromic EBT2 and EBT3 for patient-specific quality assurance: Cranial stereotactic radiosurgery using volumetric modulated arc therapy with multiple noncoplanar arcs”, *Med. Phys.* **40**, 082105 (2013).

[18]S-T. Chiu-Tsao and M. F. Chan, “Evaluation of two-dimensional bolus effect of immobilization/support devices on skin doses: A radiochromic EBT film dosimetry study in phantom”, *Med. Phys.* **37**, 3611 (2012).

[19]C. Huet, S. Dagois, S. Derreumaux, F. Trompier, C. Chenaf and I. Robbes, “Characterization and optimization of EBT2 radiochromic films dosimetry system for precise measurements of output factors in small fields used in radiotherapy”, *Radia. Meas.* **47**, 40-49 (2012).

[20]C. Bassinet, C. Huet, S. Derreumaux, G. Brunet, M. Chea, M. Baumann, T. Lacornerie, S. Gaudaire-Josset, F. Trompier, P. Roch, G. Boisserie and I. Clairand, “Small fields output factors measurements and correction factors determination for several detectors for a CyberKnife (R) and linear accelerators equipped with microMLC and circular cones”, *Med. Phys.* **40**, 071725 (2013).

[21]ICRU 74, “Patient dosimetry for x-rays used in medical imaging”, *J. Int. Comm. Radiat. Units Meas.* **5**, 29 (2005).

[22]JCGM, “Evaluation of measurement data - Guide to the expression of uncertainty in measurement (GUM 1995 with minor corrections)”, Report 100:2008, Bureau International des Poids et Mesures (2008).

[23]IEC, "Medical diagnostic x-ray equipment - radiation conditions for use in the determination of characteristics", IEC61267, International Electritechnical Commission (2005).

[24]BIPM, "Qualités de rayonnement" *CCEMRI Section I: 2nd Meeting*, R15, Bureau International des Poids et Mesures (1972)

[25]ISO, "Rayonnements X et gamma de référence pour l'étalonnage des dosimètres et des débitmetres, et pour la détermination de leur réponse en fonction de l'énergie des photons—partie 1: caractéristiques des rayonnements et méthodes de production", ISO4037-1, International Organization for Standardization (1996).

[26]B. Rapp, N. Perichon, M. Denoziere, J. Daures, A. Ostrowsky and J-M. Bordy, "The LNE-LNHB water calorimeter for primary measurement of absorbed dose at low depth in water: application to medium-energy x-rays", *Phys. Med. Biol.* **58,** 2769-2786.

[27]J. Daures, A. Ostrowsky and B. Rapp, "Small section graphite calorimeter (GR-10) at LNE-LNHB for measurements in small beams for IMRT", *Metrologia* **49,** S174-S178 (2012).

[28]F. Marsolat, D. Tromson, N. Tranchant, M. Pomorski, D. Lazaro-Ponthus, C. Bassinet, C. Huet, S. Derreumaux, M. Chea, G. Boisserie, J. Alvarez and P. Bergonzo, "Diamond dosimeter for small beam stereotactic radiotherapy", *Diam. Rel. Mat.* **33,** 63-70 (2013).

[29]F. Marsolat, D. Tromson, N. Tranchant, M. Pomorski, M. Le Roy, M. Donois, F. Moignau, A. Ostrowsky, L. De Carlan, C. Bassinet, C. Huet, S. Derreumaux, M. Chea, K. Cristina, G. Boisserie and P. Bergonzo, "A new single crystal diamond dosimeter for small beam: comparison with different commercial active detectors », *Phys. Med. Biol.* **58,** 7647-7660 (2013).

[30]L. Menegotti, A. Delana and A. Martignano, "Radiochromic film dosimetry with flatbed scanners: A fast and accurate method for dose calibration and uniformity correction with single film exposure", *Med. Phys.* **35**, 3078 (2008).

[31]B. C. Ferreira, M. C. Lopes and M. Capela, "Evaluation of an Epson flatbed scanner to read Gafchromic EBT films for radiation dosimetry", *Phys. Med. Biol.* **54,** 1073 (2009).

[32]B. D. Lynch, J. Kozelka, M. K. Ranade, J. G. Li, W. E. Simon and J. F. Dempsey, "Important considerations for radiochromic film dosimetry with flatbed CCD scanners and EBT GAFCHROMIC (R) film", *Med. Phys.* **33,** 4551-4556 (2006).

[33]A. Rink, D. F. Lewis, S. Varma, I. A. Vitkin and D. A. Jaffray "Temperature and hydration effects on absorbance spectra and radiation sensitivity of a radiochromic medium", *Med. Phys.* **35,** 4545-4555 (2008).

[34]S. Devic, J. Seuntjens, G. Hegyi, E. B. Podgorsak, C. G. Soares, A. S. Kirov, I. Ali, J. F. Williamson and A. Elizondo, "Dosimetric properties of improved GafChromic films for seven different digitizers". *Med. Phys.* **31,** 2392-2401 (2004).

[35]S. Devic, J. Seuntjens, E. Sham, , E. B. Podgorsak, C. R. Schmidtlein, A. S. Kirov and C. G. Soares, "Precise radiochromic film dosimetry using a flat-bed document scanner" *Med. Phys.* **32,** 2245-2253 (2005).

[36]J. Sorriaux, A. Kacperek, S. Rossomme, J. A. Lee, D. Bertrand, S. Vynckier and E. Sterpin, "Evaluation of Gafchromic (R) EBT3 films characteristics in therapy photon, electron and proton beams.", *Phys. Med.* **29,** 599-606 (2013).

[37]F. Salvat, J. M. Fernandez-Varea and J. Sempau, "PENELOPE-2006: A Code System for Monte Carlo Simulation of Electron and Photon Transport", Nuclear energy Agency (2006).

[38]J. E. Villarreal-Barajas and R. F. H. Khan, "Energy response of EBT3 radiochromic films: implications for dosimetry in kilovoltage range", *J.App. Clin. Med. Phys.* **15,** 331-338.

[39]J. G. H. Sutherland and D. W. O. Rogers, "Monte Carlo calculated absorbed-dose energy dependence of EBT and EBT2 film", *Med. Phys.* **37,** 1110-1116 (2010).

[40]X. G. Xu, B. Vednarz and H. Paganetti. "A review of dosimetry studies on external-beam radiation treatment with respect to second cancer induction". *Phys. Med. Biol.* **53**, 193 (2008).